Materials and Methods

C1ORF106 genetic information: C1orf106 (Gene ID: 55765; Chromosome 1, q32.1). The *333F variant refers to SNP rs41313912.

Cell culture. HEK293T cells were cultured in DMEM supplemented with 10% FBS, 2 mM L-glutamine, penicillin-streptomycin. HT29 cells were cultured in McCoy's 5A Medium supplemented with 10% FBS, 2 mM L-glutamine, penicillin-streptomycin. Cells were grown in a humidified chamber at 37°C with 5% CO_2. The human colonic Caco-2 and goblet-like LS174T cells were purchased from American Type Culture Collection (ATCC). Caco-2 cells were cultured at 70-80% confluence in Eagle's Minimum Essential Medium (EMEM) containing 20% FBS, 100 U/ml penicillin, and 100 U/ml streptomycin. LS174T cells were cultured in EMEM supplemented with 10% FBS, 100 U/ml penicillin, and 100 U/ml streptomycin. Cells were incubated in a humidified 5% CO_2 atmosphere at 37°C.

Antibodies and compounds. Antibodies were obtained as follows. R&D systems: mouse glyceraldehyde-3-phosphate dehydrogenase (686613); Santa Cruz: mouse E-cadherin antibody (H-108); Cell Signaling Technology: mouse monoclonal anti-myc (9B11), rabbit anti-E-Cadherin (24E10), anti-actin-HRP (5125S); Thermo Fisher Scientific: mouse anti-occludin (331500), mouse anti-cytohesin1 (2E11), rat anti-E-cadherin monoclonal (ECCD-2) (13-1900); Sigma Aldrich: rabbit anti-HA (H6908), rabbit anti-FLAG (F7425), rabbit anti-C1orf106 (HPA027499); Abcam: rabbit anti-C1orf106 (ab121945), β-actin (ab8227); Enzo Life Science: FK2 mouse monoclonal anti-ubiquitin; BioLegend: rabbit anti-V5 (PRB-189P); Dako: goat anti-rabbit HRP secondary (P0448), goat anti-mouse HRP secondary (P0447); Jackson ImmunoResearch: Alexa Fluor-594 rabbit anti-goat, Alexa Fluor-488 mouse anti-goat, Alexa Fluor-594 mouse anti-goat, AlexaFluor-488 rabbit anti-goat. All antibodies were used at the recommended concentrations. Pierce Streptavidin magnetic beads and Dynabeads protein G were obtained from Thermo Fisher Scientific. MG-132 was purchased from EMD Millipore. MLN4924 was obtained from Cayman Chemicals. HGF was obtained from Thermo Fisher Scientific. EZ-Link Sulfo-NHS-Biotin was obtained from Thermo Fisher Scientific. Cycloheximide was obtained from Sigma Aldrich. Concentrations used for specific experiments are described in the appropriate sections.

ARF6 activity assay. The ARF6 activity assay kit (BK033; Cytoskeleton) was used according to the manufacturer's protocol. In brief, organoids were washed with ice-cold PBS, treated with cell lysis buffer, and centrifuged at 10,000 x g at 4°C for 1 min. Supernatant was collected and protein concentration was estimated using a Bradford assay. Equal amounts of protein lysates were incubated with 20 µl GGA3-PBD beads for 1 h at 4°C on a rotator. Beads were pelleted by centrifugation at 4000 x g at 4°C for 2 min. Beads were washed twice with 600 µl wash buffer. 20 µl sample buffer was added to the beads and boiled for 2 min. The beads were spun down at 10,000 x g for 2 mins and samples were analyzed by Western blot.

Cell migration assay. An Oris cell migration assay kit (CMA1.101) was used for cell migration analysis. Cells were plated on 96-well plates and a rubber stopper was placed in the center of the well to create a space devoid of cells. Three days after plating, the stoppers were removed and images were taken at designated time intervals. Images were quantified in Microsoft PowerPoint by measuring the diameter of the cell-free zone.

Calcium chelation assay. Confluent organoid-derived monolayers were treated with 2 mM EGTA for 8 min. Fresh media was then added and confocal images were taken after 2 h. At least 10 different fields were analyzed from three independent experiments.

Immunofluorescence. Cells were washed twice with PBS, incubated in 4% (w/v) paraformaldehyde for 15 min, washed three times with PBS, and blocked with blocking buffer (5% donkey serum and 0.3% Triton-X in PBS) for 1 h at room temperature. Cells were incubated in appropriate concentrations of primary antibody in blocking buffer overnight at 4°C. Cell were washed three times in PBS and incubated with secondary antibody (1:300) in blocking buffer for 1 h. Cells were washed three times in PBS and mounted on coverslips containing Vectashield mounting medium with DAPI. LS174T cells were seeded on laminin-coated glass coverslips. Caco-2 cells were plated on collagen-coated polytetrafluoroethylene filters (Transwell, Corning) and were maintained 18 days in culture. Cells were washed with phenol red-free DMEM (Wisent) before fixation in a fresh 2% (w/v) paraformaldehyde solution for 15 min at room temperature, followed by permeabilization in a solution of 0.1% Triton X-100 (v/v) and 2% (w/v) donkey serum in PBS pH 7.2 for 30 min. Cells were immunolabeled with the primary antibodies against C1orf106 (1-2 µg/ml) and E-cadherin (4 µg/ml) overnight at 4°C and incubated with secondary host-specific anti-IgG Alexa antibodies (1:500, Invitrogen) for 1 h. Alexa Flour 594 Phalloidin was used at the recommended concentration (1:40 from 200 units/mL stock solution). Coverslips or transwells were mounted on glass slides using 0.4% (v/v) DABCO (Sigma) diluted in glycerol. Images were acquired as full Z-stacks with a LSM 510 confocal microscope (Carl Zeiss) using a 63X objective and presented as single section and orthogonal section images (XZ and YZ). Resulting images were processed using the ZEN 2012 software (Carl Zeiss, Blue edition).

Biotinylation of cell surface proteins and immunoprecipitation. Intestinal epithelial monolayers were washed with ice-cold PBS (pH 8.0) and incubated in 2 mM biotin solution in PBS at 4°C with regular shaking the plates for 45 min. Epithelial cells isolated from the intestine directly were washed with ice cold PBS (pH 8.0) and resuspended at a concentration of 25 x 10^6 cells/ml, followed by incubation in 2 mM biotin solution in PBS at 4°C with regular flicking of tubes for 45 min. Cells were washed in 100 mM glycine in PBS three times after biotin treatment. Washed cells were lysed with RIPA lysis buffer (50 mM Tris-HCl, 150 mM NaCl, 1% NP-40, 0.5% sodium deoxycholate, 0.1% SDS, pH 7.4 ± 0.2, protease inhibitors). To perform immunoprecipitation of biotinylated E-cadherin, cell lysates were incubated with streptavidin beads for 1 h at room temperature. Beads were washed three times in TBST (Tris-buffered saline (TBS), 0.1% (v/v) Tween-20) solution, eluted with 40 ml of 2X elution buffer (100 mM Tris-HCl pH 6.8, 4% SDS, 12% glycerol, 0.008% bromophenol blue, 2% β-mercaptoethanol), and boiled for 4 min.

Immunoblotting. Cells from culture dishes were rinsed with 1X PBS and the appropriate amount of RIPA lysis buffer in 4°C for 30 min. Lysates were centrifuged at 18,000 x g at 4°C for 15 min and the supernatant was collected for protein concentration estimation using a Bradford assay. Samples were prepared using 5X loading buffer (250 mM Tris-HCl pH 6.8, 10% SDS, 30% glycerol, 0.02% bromophenol blue, 5% β-mercaptoethanol) and boiled for 5 min. Samples were electrophoresed in 4-20% MP TGX polyacrylamide gels (Bio-Rad) and transferred onto PVDF using wet transfer at 80 V for 1 h. 5% nonfat dry milk in TBST was used to block the membrane for 1 h. Blots were incubated overnight at 4°C with antibody prepared in 1% milk. After three washes with TBST, the membrane was incubated with HRP-conjugated secondary antibody for 60 min at room temperature. Following secondary incubation, the blot was washed three times in TBST and incubated with chemiluminescent HRP substrate (Millipore). All Western blots were performed at least three independent times. Replicates were analyzed using ImageJ. For Caco-2 and LS174T experiments, whole protein cell extractions were carried out using a lysis buffer (50 mM Tris-HCl pH 7.6, 150 mM NaCl, 1 mM EDTA, 1% NP-40 (v/v), 1% (v/v) Triton X-100) containing a protease inhibitor mixture (Complete Mini, EDTA-Free, Roche Applied Science) and phosphatase inhibitors (5 mM NaF and 1 mM Na_3VO_4). Lysates were centrifuged at 16,000 x g at 4°C for 15 min and the supernatant protein concentrations were determined using the Pierce BCA protein assay (Thermo Fisher). Proteins were prepared in Laemmli sample buffer (Bio-Rad) and boiled for 10 min. Samples were separated by electrophoresis on an 8% denaturing polyacrylamide gel (Bio-Rad). Proteins were transferred to a nitrocellulose membrane (Bio-Rad) for immunoblotting. Membranes were incubated 30 min at room temperature in TBST supplemented with 5% (w/v) low-fat milk powder. Membranes were probed with antibodies against C1orf106 (0.2 μg/ml, 1:1000), GAPDH (0.05 μg/ml, 1:10000) or β-actin (0.33 μg/ml, 1:1000) for 1 h at room temperature in TBST containing 5% (w/v) milk powder, followed by peroxidase HRP-conjugated antibodies (Abcam, 0.5 μg/ml; 1:2000) in the same buffer. Membranes were incubated with the Western Blot Lightning Plus-ECL reagents (Perkin Elmer) according to the manufacturer's instructions. Depending on the experiment, GAPDH or β-actin was used as the loading control. Band intensity quantification was performed using ImageJ software.

Protein turnover analysis. The effective dose of cycloheximide for protein synthesis cessation was first established by performing a dose-response curve in LS174T stably overexpressing C1orf106. 50 μg/ml cycloheximide was found to significantly decrease the production of C1orf106 protein. LS174T stably overexpressing both C1orf106 alleles were seeded at 50% confluency on 6-mm Petri dishes (5.00E+05 cells/well) and grown for 16 h. Cells were then treated with EMEM medium containing 50 μg/ml cycloheximide (diluted from 10 mg/ml stock solution prepared in DMSO) for 2, 4, 8, and 16 h and washed twice with ice-cold PBS. Cell lysates were prepared and C1orf106 protein was analyzed by Western blot.

ELISA. Fecal albumin levels were detected using the mouse albumin ELISA kit from Bethyl laboratories according to the manufacturer's instruction. Fecal IgA levels were

detected using the mouse IgA kit from Thermo Fisher Scientific according to the manufacturer's instruction.

qRT-PCR. RNA was extracted and purified using RNeasy (Qiagen) and cDNA was generated using the iScript Synthesis kit (Bio-Rad). Quantitative PCR was performed using SYBR Green Supermix (Bio-Rad). Samples were run in a 25 µl mixture in the following PCR program: initial denaturation at 95 °C for 10 min, followed by 40 cycles of 95 °C for 20 s, 60 °C for 30 s, 72 °C for 1 min, and a final extension at 72 °C for 10 min. The following primers were used for the specific genes:

C1orf106MusFor: CAGACTACCTACACATCCTGGC
C1orf106MusRev: TCAGCTCTTTCATTGGAGAGACA

BTRC1HomoFor: CCAGACTCTGCTTAAACCAAGAA
BTRC1HomoRev: GGGCACAATCATACTGGAAGTG

FBXW11HomoFor: GGAACATCATCTGTGATCGTCTC
FBXW11HomoRev: TGGTAAAGCGGTAATAAAGTCCC

Claudin1MusFor: ATGGCCAACGCGGGGCTG
Claudin1MusRev: TTCCCACTAGAAGGTGTTGGC

OccludinMusFor: TGGCAAGCGATCATACCCAG
OccludinMusRev: CCTCTTGCCCTTTCCTGCTT

Caludin2MusFor: CAACTGGTGGGCTACATCCTA
Claudin2MusRev: ATCCAGAGGCCCTTGGAAAAG

ZO-1MusFor: TTCAAAGTCTGCAGAGACAATAGC
ZO-1MusRev: TCACATTGCTTAGTCCAGTTCC

F4/80MusFor: CTGCACCTGTAAACGAGGCTT
F4/80MusRev: GCAGACTGAGTTAGGACCACAA

IL22MusFor: ATGAGTTTTTCCCTTATGGGGAC
IL22MusRev: GCTGGAAGTTGGACACCTCAA

LipocalinMusFor: TGGCCCTGAGTGTCATGTG
LipocalinMusRev: CTCTTGTAGCTCATAGATGGTGC

Reg3AMusFor: ATGGGTTACAAGGCTTATCGC
Reg3AMusRev: AGAATAGACACGAGATGTCCTGA

Reg3BMusFor: CCCTCCGCACGCATTAGTT
Reg3BMusRev: CAGGCCAGTTCTGCATCAAA

Reg3GMusFor: ATGCTTCCCCGTATAACCATCA
Reg3GMusRev: ACTTCACCTTGCACCTGAGAA

CRIS1CMusFor: CACCACCCAAGCTCCAAATACACAG
CRIS1CMusRev: ATCGTGAGGACCAAAAGCAAATGG

Defcr24MusFor: TCAAGAGGCTGCAAAGGAAGAGAAC
Defcr24MusRev: TGGTCTCCATGTTCAGCGACAGC

Lyz1MusFor: GGCTGGCTACTATGGAGTCAGCCTG
Lyz1MusRev: GCATTCACAGCTCTTGGGGTTTTG

sPLA1MusFor: AGGATTCCCCCAAGATGCCAC
sPLA1MusRev: CAGCCGTTTCTGACAGGAGTTCTGG

Lyz2MusFor: GGCTGGCTACTATGGAGTCAGCCTG
Lyz2MusRev: GCATTCACAGCTCTTGGGGTTTTG

CYTH1MusFor: CTGACATCCAGAGGCTAAAGGA
CYTH1MusRev: CAGGCCATTCTCGATTAAGAACT

CYTH2MusFor: ATGGAGGACGGTGTCTACGAG
CYTH2MusRev: TTCCGCTGCAAGGTCTTACTG

CYTH3MusFor: AGGAGAGGGCCTGAACAAGA
CYTH3MusRev: GCCTGGACAAGGTTGAGATCA

Transfection. Cells were transfected at 70-80% confluency using FuGENE HD (Promega) according to the manufacturer's instructions.

Co-immunoprecipitation. Cells were rinsed with 1X PBS and lysed using RIPA. For immunoprecipitation using protein G beads, cell lysates were incubated with antibody for 1 h at 4°C. Lysate/antibody mixtures were incubated with 40 µL protein A Dynabeads (Invitrogen; prewashed in PBS and lysis buffer) for 1 h at 4°C. After 3 h, lysate/antibody bead mixtures were washed three times using 200 µL RIPA. After washing, proteins were eluted at 100°C for 5 min with 2X reaction buffer (100 mM Tris-HCl, pH 6.8, 4% SDS, 12% glycerol, 0.008% bromophenol blue, 2% β-mercaptoethanol). For immunoprecipitation using streptavidin beads, cell lysates were incubated with 20 µl beads and incubated for 1 h at 4°C on a rotator. Beads were washed three times in RIPA and eluted as described above. Samples for the ubiquitination assay were prepared by lysing cells with RIPA, and excess SDS was added to bring the total SDS concentration to 1%. Lysates were boiled for 5 min at 100°C. SDS-free lysis buffer was added to bring back the total concentration to < 0.1%. Samples were centrifuged at 18,000 x g at 4°C and the supernatant was collected. Eluates were electrophoresed in 4-20% MP TGX polyacrylamide gels (Bio-Rad) and analyzed by Western blotting.

Lentiviral particle production and transduction of LS174T and Caco-2 cells. All shRNA vectors were obtained from Sigma (MISSION). C1orf106 shRNA (TRCN0000140233), shRNA empty control vectors (SHC001V), and pLVX-EF1a-IRES-puro/eGFP-C1orf106*Y333 or pLVX-EF1a-IRES-puro/eGFP-C1orf106*333F vectors were added to lentiviral packaging and envelope vectors (Sigma, MISSION) in a ratio of 2:2:1. Vector mixtures were transfected in HEK293T cells by calcium phosphate precipitation according to the Open Biosystems protocol. 48 h after transfection, lentivirus-containing medium was collected, cell debris pelleted, and the supernatant filtered through a 0.45 μm filter. The resulting supernatants were used to transduce low passage (5-10) LS174T Caco-2 cells. ORF-containing lentiviral particles were concentrated using the Lenti-X concentrator reagent from Clontech and resuspended in DMEM medium. shRNA lentiviral particles titers were determined by the QuickTiter Lentivirus-Associated p24 Titer Kit (Cell Biolabs) according to the manufacturer's protocol. Effective titration of ORF-containing lentivirus was determined by $eGFP^+$ cell counts of HT-29 cells transduced with serial-diluted viral stocks using the IN cell Analyzer 6000 Cell imaging system (GE Healthcare Life Sciences). Cells were seeded at 50% confluency 24 h prior to infection with lentiviral particles at an MOI of ~10 in EMEM containing 1% FBS and 8 μg/mL polybrene (minimal medium). Lentivirus-containing medium was removed 24 h later and replaced with minimal medium for an additional 24 h, before launching the selection of transduced cells with the addition of an effective dose of puromycin to the cell culture medium. Transduced Caco-2 cells were selected for at least two cell passages in puromycin-containing (10 μg/ml) medium. LS14T cells were selected in 3 μg/ml puromycin for three days. Once the selection was completed, total RNA and protein were extracted to confirm knockdown or overexpression of C1orf106.

RNA expression analyses; microarray. Expression levels of *C1orf106* in 14 different human tissues (bone marrow, heart, skeletal muscle, uterus, liver, fetal liver, spleen, thymus, thyroid, prostate, brain, lung, small intestine, and colon) purchased from Clontech Laboratories were determined using a custom expression array from Agilent, containing one probe for each exon of all 2,982 candidate genes involved in autoimmune and inflammatory diseases including IBD, celiac disease, systemic lupus erythematous, and multiple sclerosis. Additionally, housekeeping genes (~40), differentiation markers of the cell lines used (~150), and genes associated with cardiovascular diseases (~150) were included. A reference RNA sample comprised of an admixture of 10 different human tissues (adrenal gland, cerebellum, whole brain, heart, liver, prostate, spleen, thymus, colon, and bone marrow) was also included in the analyses. All RNA samples tested had a RNA Integrity Number (RIN) ≥ 8 (range 8.0-9.3), as measured by Agilent 2100 Bioanalyzer using the RNA Nano 6000 kit (Agilent Technologies), with the exception of the small intestine (RIN = 7.6). Labeled complementary RNA (cRNA) was synthesized from 50 ng total RNA samples using a Low Input Quick Amp WT labeling kit (Agilent Technologies) according to the manufacturer's protocol. Quantity and quality of labeled cRNA samples were assessed by NanoDrop UV-VIS Spectrophotometer. Sample hybridization was performed according to the manufacturer's standard protocol and microarrays were scanned using the Sure Scan Microarray Scanner (Agilent

Technologies). An expression value was obtained for each sample (or measurement) by calculating the geometric mean of all probes within the gene, followed by a median normalization across all genes on the array. A geometric mean and standard deviation was calculated from at least 3 independent measurements for each tissue.

Extended proteomics methods for C1orf106-protein interaction studies. *On-bead digest.* The beads from immunopurification were washed once with IP lysis buffer, then three times with PBS. Three different lysates of each replicate were resuspended in 90 µL digestion buffer (2 M Urea, 50 mM Tris HCl), 2 µg of sequencing grade trypsin was added and then shaken for 1 h at 700 rpm. The supernatant was removed and placed in a fresh tube. Beads were washed twice with 50 µL digestion buffer and combined with the supernatant. The combined supernatants were reduced (2 µL 500 mM DTT, 30 min, room temperature), alkylated (4 µL 500 mM IAA, 45 min, dark) and a longer overnight digestion performed with 2 µg (4 µL) trypsin, shaking overnight. The samples were then quenched with 20 µL 10% FA and desalted on 10-mg Oasis cartridges.

iTRAQ labeling of peptides and strong cation exchange (scx) fractionation. Desalted peptides were labeled with iTRAQ reagents according to the manufacturer's instructions (AB Sciex). Peptides were dissolved in 30 µl of 0.5 M TEAB pH 8.5 solution and labeling reagent was added in 70 µl ethanol. After 1 h incubation, the reaction was stopped with 50 mM Tris/HCl pH 7.5. Differentially labeled peptides were mixed and subsequently desalted on 10-mg Oasis cartridges.

	iTRAQ labeling			
	114	115	116	117
Rep1	WT	Empty Vector	Empty Vector	Mutant
Rep2	WT	Empty Vector	Empty Vector	Mutant

Channels 115 and 117 were not used in this manuscript

SCX fractionation of the differentially labeled and combined peptides was performed as previously described (*20*) with 6 pH steps (buffers all contain 25% acetonitrile) as listed below:

1: ammonium acetate 50 mM pH 4.5
2: ammonium acetate 50 mM pH 5.5
3: ammonium acetate 50 mM pH 6.5
4: ammonium bicarbonate 50 mM pH 8
5: ammonium hydroxide 0.1% pH 9
6: ammonium hydroxide 0.1% pH 11

MS analysis. Reconstituted peptides were separated on an online nanoflow EASY-nLC 1000 UHPLC system (Thermo Fisher Scientific) and analyzed on a benchtop Orbitrap Q Exactive mass spectrometer (Thermo Fisher Scientific). The peptide samples were injected onto a capillary column (Picofrit with 10 µm tip opening / 75 µm diameter, New Objective, PF360-75-10-N-5) packed in-house with 20 cm C18 silica material (1.9 µm

ReproSil-Pur C18-AQ medium, Dr. Maisch GmbH, r119.aq). The UHPLC setup was connected with a custom-fit microadapting tee (360 μm, IDEX Health & Science, UH-753), and capillary columns were heated to 50°C in column heater sleeves (Phoenix-ST) to reduce backpressure during UHPLC separation. Injected peptides were separated at a flow rate of 200 nL/min with a linear 80 min gradient from 100% solvent A (3% acetonitrile, 0.1% formic acid) to 30% solvent B (90% acetonitrile, 0.1% formic acid), followed by a linear 6 min gradient from 30% solvent B to 90% solvent B. Each sample was run for 120 min, including sample loading and column equilibration times. The Q Exactive instrument was operated in the data-dependent mode acquiring HCD MS/MS scans (R = 17,500) after each MS1 scan (R = 70,000) on the 12 most abundant ions using an MS1 ion target of 3 x 10^6 ions and an MS2 target of 5 x 10^4 ions. The maximum ion time utilized for the MS/MS scans was 120 msec; the HCD-normalized collision energy was set to 27; the dynamic exclusion time was set to 20 s, and the peptide match and isotope exclusion functions were enabled.

Quantification and identification of peptides and proteins. All mass spectra were processed using the Spectrum Mill software package v6.0 pre-release (Agilent Technologies), which includes modules we developed for iTRAQ-based quantification. Precursor ion quantification was performed using extracted ion chromatograms (XICs) for each precursor ion. The peak area for the XIC of each precursor ion subjected to MS/MS was calculated automatically by the Spectrum Mill software in the intervening high-resolution MS1 scans of the LC-MS/MS runs using narrow windows around each individual member of the isotope cluster. Peak widths in both the time and *m*/*z* domains were dynamically determined based on MS scan resolution, precursor charge and *m*/*z,* subject to quality metrics on the relative distribution of the peaks in the isotope cluster vs theoretical. Similar MS/MS spectra acquired on the same precursor *m/z* in the same dissociation mode within ± 60 sec were merged. MS/MS spectra with precursor charge >7 and poor quality MS/MS spectra, which failed the quality filter by not having a sequence tag length > 1 (i.e., minimum of 3 masses separated by the in-chain mass of an amino acid), were excluded from searching.

For peptide identification, MS/MS spectra were searched against human Uniprot database to which a set of common laboratory contaminant proteins was appended. Search parameters included ESI-QEXACTIVE-HCD scoring parameters, trypsin enzyme specificity with a maximum of two missed cleavages, 40% minimum matched peak intensity, ± 20 ppm precursor mass tolerance, ± 20 ppm product mass tolerance, and carbamidomethylation of cysteines and iTRAQ labeling of lysines and peptide N-termini as fixed modifications. Allowed variable modifications were oxidation of methionine, N-terminal acetylation, pyroglutamic acid (N-term Q), deamidated (N), pyro carbamidomethyl Cys (N-term C), with a precursor MH+ shift range of -18 to 64 Da. Identities interpreted for individual spectra were automatically designated as valid by optimizing score and delta rank1-rank2 score thresholds separately for each precursor charge state in each LC-MS/MS while allowing a maximum target-decoy-based false-discovery rate (FDR) of 1.0% at the spectrum level.

In calculating scores at the protein level and reporting the identified proteins, redundancy is addressed in the following manner: the protein score is the sum of the scores of distinct peptides. A distinct peptide is the single highest scoring instance of a peptide detected through an MS/MS spectrum. MS/MS spectra for a particular peptide may have been recorded multiple times (i.e., as different precursor charge states, isolated from adjacent SCX fractions, modified by oxidation of Met), but are still counted as a single distinct peptide. When a peptide sequence > 8 residues long is contained in multiple protein entries in the sequence database, the proteins are grouped together and the highest scoring one and its accession number are reported. In some cases when the protein sequences are grouped in this manner, there are distinct peptides that uniquely represent a lower scoring member of the group (isoforms or family members). Each of these instances spawns a subgroup and multiple subgroups are reported and counted towards the total number of proteins. iTRAQ ratios were obtained from the protein-comparisons export table in Spectrum Mill. To obtain iTRAQ protein ratios the median was calculated over all distinct peptides assigned to a protein subgroup in each replicate. To assign interacting proteins, we used the Limma package in the R environment to calculate moderated *t*-test *p*, as described previously (*21*).

Mice. All experiments involving mice were carried out according to protocols approved by the Subcommittee on Research Animal Care at Massachusetts General Hospital and were performed with littermate controls including both male and female mice. Mice were maintained in specific-pathogen-free facilities at Massachusetts General Hospital. The *C1orf106*$^{-/-}$ strain was developed at inGenious Targeting Laboratory. Targeted iTL BA1 (C57BL/6 x 129/SvEv) hybrid embryonic stem cells were microinjected into C57BL/6 blastocysts. Resulting chimeras with a high percentage agouti coat color were mated to wild-type C57BL/6N mice to generate F1 heterozygous offspring. *C1orf106*$^{-/-}$ mice are viable and born in Mendelian ratios. The targeted locus spans exon 2 and exon 8 of *C1orf106* (Fig. S2A). Knockout was confirmed by Southern blot and Western blot.

Citrobacter rodentium **infection**. Bacteria were cultured in 10 ml media overnight and subcultured in 50 ml media the following day until the OD reached 1.46. Cultures were centrifuged at 4000 rpm for 10 min, and pellets were resuspended in 5 ml PBS. 100 µl of resuspended culture, containing approximately 5 x 10^9 bacteria, was used to gavage each mouse. Mice were deprived of food and water for 3 h before infection. Water was provided soon after gavage, and food was supplied 3 h after gavage. After 5 days, bacterial loads were detected using a bioluminescence illuminator. Stool, MLN, and spleen were processed in PBS using bead beating, and dilutions were plated on LB plates. Colonies were counted manually to determine bacterial concentrations. Histological slides were scored blinded using the following criteria, with a maximum possible score of 10 per sample slide. Inflammation, hyperplasia, edema, and epithelial damage were assessed. Inflammation/cellular infiltration was scored on a scale of 0-3 with normal = 0; mild = 1; moderate = 2; or severe = 3. Hyperplasia was scored on a scale of 0-3 with 0-100% (normal mucosal thickness) = 0; 100-150% = 1; 150-200% = 2; and >200% = 3. Edema was scored on a scale of 0-2. Epithelial damage was scored on a scale of 0-2 with no epithelial damage = 0; surface epithelial damage only = 1; and epithelial damage penetrating to the crypt base = 2. Each mouse was scored. For cytokine analysis, distal

colon tissues were harvested and cultured overnight in RPMI with 10% serum and penicillin/streptomycin. For protein cytokine analysis, supernatants were harvested and centrifuged at high speed to remove cellular debris. Cytokines were quantified using cytokine bead array mouse flex sets (BD Biosciences) according to the manufacturer's protocol.

Intestinal permeability assays. FITC-Dextran. Mice used for the experiments were deprived of food and water overnight. On the following day, FITC-dextran (4KDa) dissolved in PBS at a concentration of 44 mg/100 g body weight was administered by oral gavage. After 3 h blood was collected from the mice, and FITC level in the serum was estimated by spectrophotometer with an excitation of 485 nm and an emission wavelength of 528 nm (*22*). **Lucifer Yellow.** Intestinal sections of 5 weeks old mice were cut longitudinally, and muscle layers were carefully removed mechanically. Epithelial layers were placed on Snapwell chambers sandwiched between 0.4 μm pore polycarbonate membranes and supported by a detachable ring. 1 mM Lucifer yellow dissolved in phenol red-free DMEM was added on the top chamber. Phenol red-free DMEM was added on the lower chamber. 100 μL of DMEM was collected from the lower chamber, and Lucifer yellow levels were determined at an excitation wavelength of 428 nm by a microplate reader. Permeability was calculated using the following formula: $P_{app} = (dQ/dt)(1/A\ C_0\ 60)$(cm/s). ($dQ/dt$) = amount of substance transported per min (ng/min or RFU); A = surface area of filter (cm^2), C_0 = starting concentration of substance (ng/mL), 60 = conversion of min to sec (*23*).

DSS-induced colitis. Mice were provided with 2.25% (w/v) dextran sodium sulfate (DSS) (molecular weight 36,000–50,000; MP Biomedicals, Solon, OH) dissolved in sterile drinking water ad libitum. Animal weights were monitored every day. Mice were euthanized if the body weight does not improve 24 hours after a 15% body weight loss. Histological slides were scored blinded using the following criteria, with a maximum possible score of 10 per sample slide (*24*). The following independent parameters were measured: severity of inflammation, depth of injury/inflammation, and crypt damage. Severity was scored on a scale of 0-3 with none = 0; slight = 1; moderate = 2; or severe = 3. Depth of injury/inflammation was scored on a scale of 0-3 with none = 0, mucosal = 1, submucosal = 2, and transmural = 3. Epithelial damage was scored on a scale of 0-4 with no epithelial damage = 0; basal one-third damaged = 2, basal two-third damaged = 2, only surface epithelium intact = 3, or entire crypt and epithelium lost = 4. These changes were also quantified by the percentage of the tissue involved. That is, the score of each parameter was multiplied by a factor reflecting the percentage of tissue involvement: 0-25% = x 1; 26-50% = x 2; 51-75% = x 3; and 76-100% = x 4. Each section was then scored for each feature separately by establishing the product of the grade for that feature and the percentage involvement (ranging from 0 to 12 for severity and depth of inflammation and from 0 to 16 for crypt damage). The products were added to a sum. The maximum possible score is 40. The histological injury was the sum of the scores obtained from three sections, each taken from the proximal, middle, and distal portions of the colon. The maximal histological injury score is 120 (*25*). The numbers were plotted on a scale of 0-12.

Immunophenotyping. Intestine sections were flushed with PBS and then incubated with epithelial strip buffer (HBSS, 5 mM EDTA, 1 mM DTT, 15mM Hepes, 5% FCS) for 30 minutes at 37ºC with shaking. Tissues were washed 3 times with 15-20 ml HBSS prior to being digested with 150 ug/mL Liberase TL (Roche brand, Catalog# 05401020001) containing 0.1 mg/mL DNase for 30 minutes at 37ºC with shaking. To stop the reaction, cold HBSS (with 5% FBS and 1mM EDTA) was added the digested tissue, which was then placed on ice. Single cell suspensions were obtained by filtering digested tissue through a 100 μM nylon filter. Lamina propria cells were enriched by Percoll gradient centrifugation. Lamina propria cells were stained with fluorescent-conjugated antibodies and analyzed using a BD LSR II flow cytometer. Fluorescent-conjugated antibodies against mouse CD11b, CD11c, IA-IE, Gr-1, Ly6G, CD64, TCRb, TCRgd, CD5, CD4, CD8, B220, CD90.2, and CD45 were obtained from eBioscience and Biolegend. Anti-mouse Siglec F antibody was obtained from BD Biosciences.

Plasmids. C1orf106 WT and C1orf106 Y333F (NM_018265) were obtained from Genescript in pLX_TRC304-V5 lentiviral vector. For other C1orf106 and the variant constructs, the ORF was cloned into pcDNA4/TO-FLAG-StrepII. 1-1182 bp constitute the N-terminal domain of C1orf106; 414-1737 bp constitute the C-terminal domain. Cytohesin-1 and 2 were obtained from Genetic Perturbation Platform of Broad Institute. For other cytohesin-1 constructs, ORFs were cloned into pcDNA4/TO-FLAG-StrepII and pCMV-3xHA vectors. 1-204 bp constitute the N-terminal domain of cytohesin-1; 216-1194 bp constitute the C-terminal domain. 1-213 bp and 192-1203 bp of cytohesin-2 constitute the N- and C-terminal domains respectively. Domains were cloned into pcDNA4/TO-FLAG-StrepII. Ubiquitin cDNA was kindly provided by Dr. M. Scheffner (University of Konstanz, Germany). p4489 FLAG-betaTrCP was a gift from Peter Howley (Addgene plasmid 10865). NC14 pGLUE FBXW11 was a gift from Randall Moon (Addgene plasmid 36969). pcDNA3-myc3-CUL1 was a gift from Yue Xiong (Addgene plasmid 19896). SKP1 plasmid was obtained from Genetic Perturbation Platform of Broad Institute. C1orf106 ORF nucleotide sequence (C1orf106-opt) was designed and synthesized by GeneArt (Thermo Fisher) using GeneOptimizer software to optimize gene expression. This DNA fragment was cloned into a pENTR^{-}221 vector compatible for Gateway cloning. To generate C1orf106 *333F, the C1orf106-opt sequence was modified by replacing Tyr^{333} with phenylalanine (C1orf106*333F-opt) and swapped by StuI digestion into the pENTRY-221-C1orf106-opt plasmid. Both alleles were then transferred into the destination pLVX-EF1a-IRES-puro/eGFP vector using the Gateway LR recombination system (Thermo Fisher). shRNA against cytohesin1 (TRCN0000110118) was obtained from Genetic Perturbation Platform of Broad Institute. The control shRNA was pLKO1. All plasmid constructs were validated by Sanger sequencing using a 3730xl DNA Analyzer at the Génome Québec/McGill University Innovation Center and DNA sequences analyzed using CLC DNA Workbench software (Qiagen).

Organoid culture. Colonic organoids were isolated and cultured as previously described (*26*). Briefly, crypts were isolated from mice by incubation of colonic tissue in 8 mM EDTA in PBS for 60-90 min at 4°C, followed by manual disruption of the tissue by pipetting. Crypts were plated in 30 μl Matrigel basement membrane (Corning) and

maintained in 50% L-WRN media (50% L-WRN conditioned media (*26*) diluted with advanced DMEM F-12 supplemented with 10% FBS, GlutaMAX, and penicillin-streptomycin). Crypts typically form colonic organoids within 24 h of plating in Matrigel. For passaging, organoids were lifted into PBS and broken down into small cell clusters with TryplE followed by manual disruption using a P1000 pipet. Cell clusters were resuspended in Matrigel and plated in fresh plates. Media was replaced every 2 days, and organoids were passaged every 3-4 days. Differentiation of colonic organoids into a 2D monolayer culture has been previously described (*27*). Briefly, organoids were broken down to a single-cell suspension using TryplE and passed through a 40 μm filter to remove large clusters of cells. Single cells were suspended in 50% L-WRN media supplemented with 10 μM Y27632 (R&D Systems). The single-cell suspension was plated at a density of 4.3 x 10^5 cells per cm^2 in wells coated with a thin layer of Matrigel. After 24 h, the media was replaced with 50% L-WRN lacking Y26732. After an additional 24 h, the media was replaced with 5% L-WRN to induce differentiation. Media was replaced daily, and monolayers were maintained for up to 7 days.

Trans-epithelial electrical resistance (TEER). Caco-2 cells were grown as monolayers on collagen-coated polytetrafluoroethylene filters (Transwell, Corning) and were maintained 18 days in culture with medium changes every two days. Monolayers derived from organoids were cultured on transwell dishes, and TEER was measured daily until maximal TEER was attained. TEER was determined by measuring the resistance across the monolayer using chopstick electrodes and Millicell ERS-2 Voltohmmeter (Millipore). The resistance value, measured in ohms (Ω), was obtained by subtracting the TEER value of the blank insert and multiplying the difference by the growth surface area of the filter. Filters were also used for confocal microscopy.

Virus transduction of organoids. This procedure was performed according to Koo et al., 2012 with some modifications. Concentrated virus was resuspended in infection media (*28*). Organoids from 5 wells were harvested, centrifuged at 400 x g for 5 min, and digested using 500μL of TryEL (Invitrogen). After 4 min of incubation at 37ºC, cells were pipetted 7 times, supplemented with 5 ml of basal media, and centrifuged for 800 x g for 5 min. Pellets were resuspended in 250μL of viral suspension media and transferred to 48-well plates. Plates were centrifuged at 600 x g for 90 min at 30ºC. After 2 hours of incubation in a tissue culture incubator at 37ºC, cells were collected in an eppendorf tube and centrifuged at 900 x g for 5 min. Cells were resuspended in 75μL of Matrigel, and a 15 μL drop was plated in a 24-well dish. 0.5 ml of 50% L-WRN plus Y27632 media was added to each well. Organoid growth was monitored over the next 2-5 days (*28*).

Statistical analysis. Each experiment was completed in at least three biological replicates. Western blots were performed on separate cell lysates at least three times. Student's t test or Welch's t test was used to analyze difference between two groups. $*P< 0.05$ was considered significant. To compare more than 2 groups, a one-way ANOVA was used with multiple comparisons testing. For microarray analysis, the expression data was processed using GeneSpring (version 12.5). Probe fluorescence intensity was corrected to remove background, and gene expression summary was computed as the geometric mean of probe expression. Expression data were normalized by the median and

for each condition. Summary statistics per gene were computed as geometric mean and geometric standard deviation (R 3.01). For TEER analysis, we used the TEER values at every time point to estimate the maximum plateau considering that each sample might grow at different rates. TEER values were log transformed to account for increased variance at higher values and to model multiplicative effects. Technical replicates were pooled together. A sigmoid (four parameter logistic) curve was fitted to the log(TEER) vs. time data for each independent sample. The estimated top plateau was obtained from the fit and used in further analyses and comparisons. Graphical display was used to assess quality of the fit.

Table S1 (separate file). List of C1orf106 interactors from iTRAQ proteomic analysis.

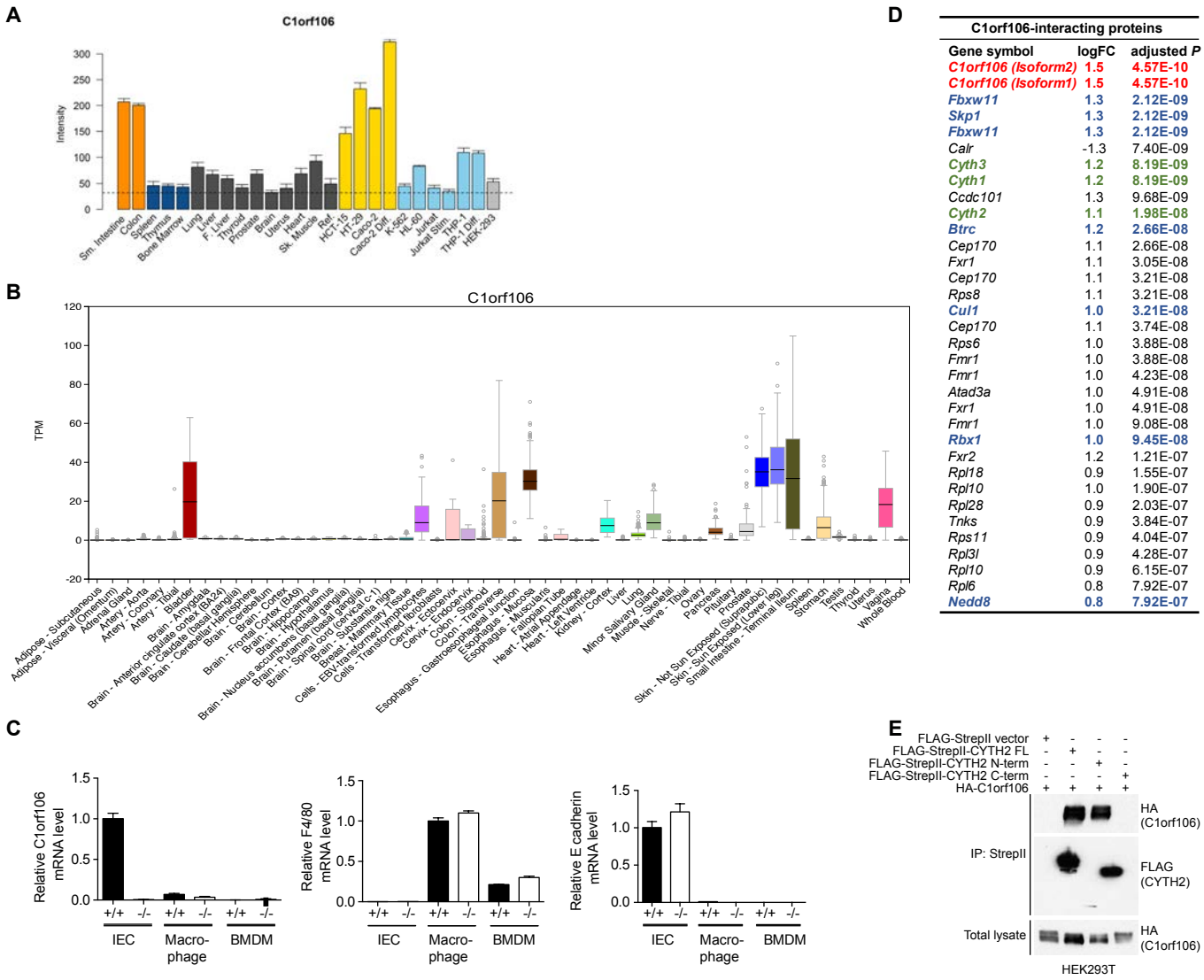

D

C1orf106-interacting proteins		
Gene symbol	**logFC**	**adjusted *P***
C1orf106 (Isoform2)	1.5	4.57E-10
C1orf106 (Isoform1)	1.5	4.57E-10
Fbxw11	1.3	2.12E-09
Skp1	1.3	2.12E-09
Fbxw11	1.3	2.12E-09
Calr	-1.3	7.40E-09
Cyth3	1.2	8.19E-09
Cyth1	1.2	8.19E-09
Ccdc101	1.3	9.68E-09
Cyth2	1.1	1.98E-08
Btrc	1.2	2.66E-08
Cep170	1.1	2.66E-08
Fxr1	1.1	3.05E-08
Cep170	1.1	3.21E-08
Rps8	1.1	3.21E-08
Cul1	1.0	3.21E-08
Cep170	1.1	3.74E-08
Rps6	1.0	3.88E-08
Fmr1	1.0	3.88E-08
Fmr1	1.0	4.23E-08
Atad3a	1.0	4.91E-08
Fxr1	1.0	4.91E-08
Fmr1	1.0	9.08E-08
Rbx1	1.0	9.45E-08
Fxr2	1.2	1.21E-07
Rpl18	0.9	1.55E-07
Rpl10	1.0	1.90E-07
Rpl28	0.9	2.03E-07
Tnks	0.9	3.84E-07
Rps11	0.9	4.04E-07
Rpl3l	0.9	4.28E-07
Rpl10	0.9	6.15E-07
Rpl6	0.8	7.92E-07
Nedd8	0.8	7.92E-07

Fig. S1. C1orf106 is highly expressed in epithelial cells and interacts with cytohesins. (**A**) Expression levels of *C1orf106* in a panel of human tissues (bone marrow, heart, skeletal muscle, uterus, liver, fetal liver, spleen, thymus, thyroid, prostate, brain, lung, small intestine, and colon) and human cell lines using a custom Agilent expression array. Cell lines represent models of human T lymphocytes (Jurkat), monocytes (THP-1), erythroleukemia cells (K562), promyelocytic cells (HL-60), colonic epithelial cells (HCT-15, HT-29, Caco-2), and cells from embryonic kidney (HEK293). In addition, models of differentiated colonic epithelium (Caco-2 differentiated for 21 days in culture [Caco-2 diff]), activated T lymphocytes (Jurkat cells stimulated with PMA [40 ng/ml] and ionomycin [1 µg/ml] for 6 h [Jurkat stim]), and macrophages (derived from THP-1 differentiated for 24 h [THP-1 diff] with IFN γ [400 U/ml] and TNFα [10 ng/ml]) were examined. Intensity values for each tissue/cell line represent the geometric mean with geometric standard deviation of 3 independent measurements; each measurement represents the geometric mean of all probes (one per exon) for each gene followed by a median normalization across all genes on the array. Dotted line indicates the threshold level for detection of basal expression. The reference sample is composed of a mixture of RNAs derived from 10 different human tissues. (**B**) Expression profile of C1orf106 in different types of tissues. Data is obtained from GTEx database. (**C**) qRT-PCR analysis of C1orf106 in different cell types isolated from *C1orf106*$^{+/+}$ and *C1orf106*$^{-/-}$ mice. Data are representative of 3 independent experiments. (**D**) Proteins identified by MS analysis as significantly enriched after C1orf106 immunoprecipitation. Fold change (FC) enrichment of proteins compared to cells transfected with empty vector and adjusted *P* value are shown. (**E**) HEK293T cells were transiently transfected with HA-C1orf106 and either empty vector, full-length FLAG-StrepII-CYTH2 or the N- or C-terminal domains of CYTH2. Samples were immunoprecipitated with anti-StrepII and probed for FLAG (CYTH2) and HA (C1orf106).

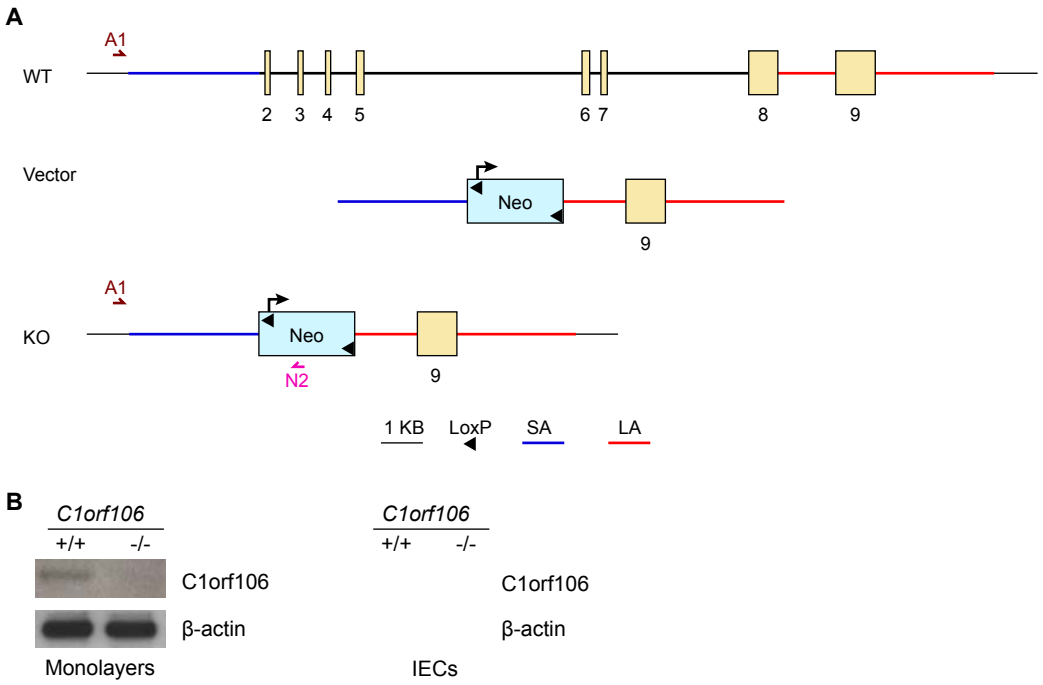

Fig. S2. Generation of *C1orf106*$^{-/-}$ mice. (**A**) Schematic illustrating the *C1orf106* gene targeting strategy designed by inGenious Targeting Laboratory. A1, N2, genotyping primers; SA, short homology arm; LA, long homology arm. The KO mice generated were crossed with CMV-cre mice to remove Neo sequence. (**B**) Immunoblot analysis of intestinal epithelial monolayers derived from organoids and intestinal epithelial cells (IECs) isolated from the colon of C1orf106$^{+/+}$ and C1orf106$^{-/-}$ mice and probed for C1orf106 and β-actin.

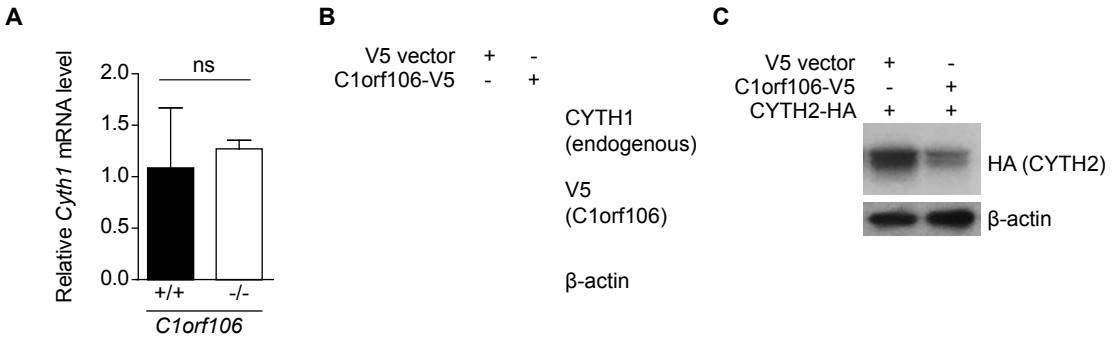

Fig. S3. C1orf106 controls the levels of cytohesin protein. (**A**) qRT-PCR analysis of cytohesin-1 levels in organoids derived from *C1orf106*$^{+/+}$ and *C1orf106*$^{-/-}$ mice. ns, not significant, Student's t test. Error bars represent SD. (**B**) Immunoblot analysis of HEK293T cells transfected with empty vector or C1orf106-V5 and probed for endogenous cytohesin-1. β-actin served as a loading control. (**C**) Immunoblot analysis of HEK293T cells co-transfected with cytohesin-2-HA and either empty vector or C1orf106-V5 and probed for cytohesin-2 using anti-HA antibody. β-actin served as a loading control.

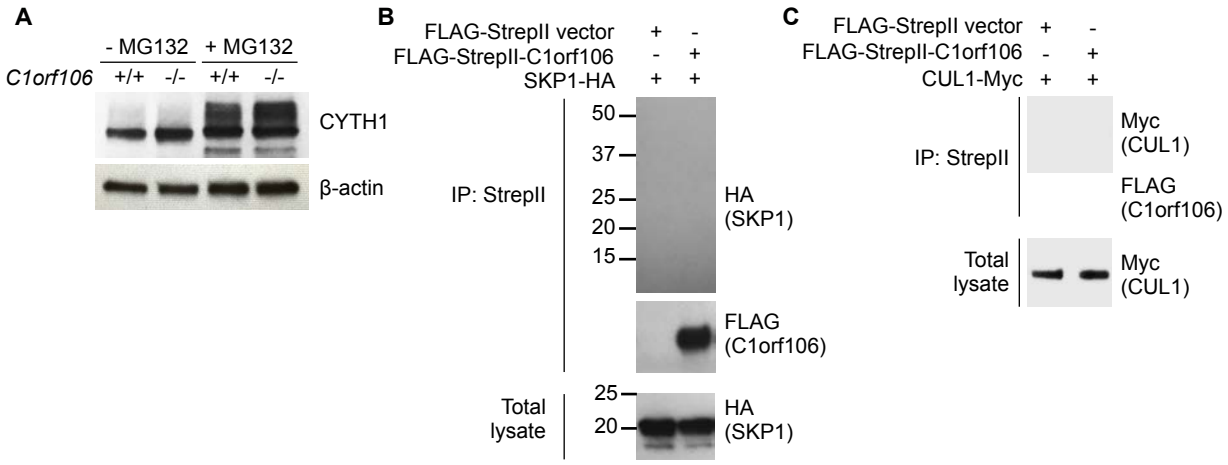

Fig. S4. C1orf106 and the SCF ubiquitin ligase complex. (**A**) Immunoblot analysis of organoids from *C1orf106*$^{+/+}$ and *C1orf106*$^{-/-}$ mice treated with MG132 or DMSO and probed for cytohesin-1. β-actin served as a loading control. (**B**) HEK293T cells were transiently transfected with SKP1-HA and either empty vector or full-length FLAG-StrepII-C1orf106. Samples were immunoprecipitated with anti-StrepII and probed for FLAG (C1orf106) and HA (SKP1). (**C**) HEK293T cells were transiently transfected with CUL1-Myc and either empty vector or full-length FLAG-StrepII-C1orf106. Samples were immunoprecipitated with anti-StrepII and probed for FLAG (C1orf106) and Myc (CUL1).

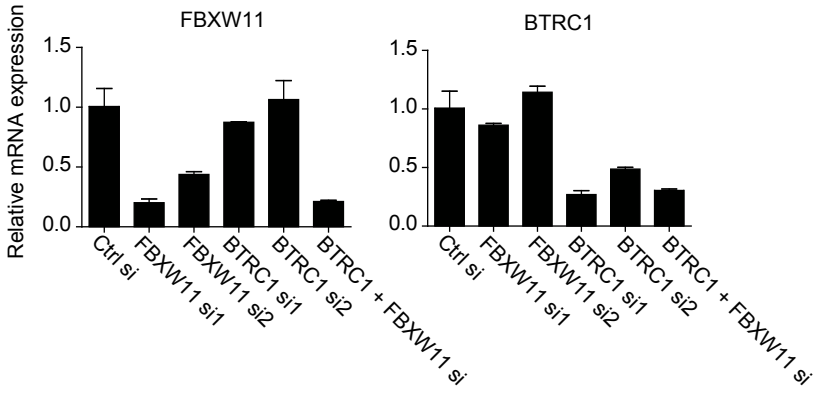

Fig. S5. Efficacy of siRNAs against FBXW11 and BTRC1. qRT-PCR analysis of *FBXW11* and *BTRC1* in HEK293T cells transfected with control siRNA or siRNA against FBXW11 and/or BTRC1. Error bars represent SD.

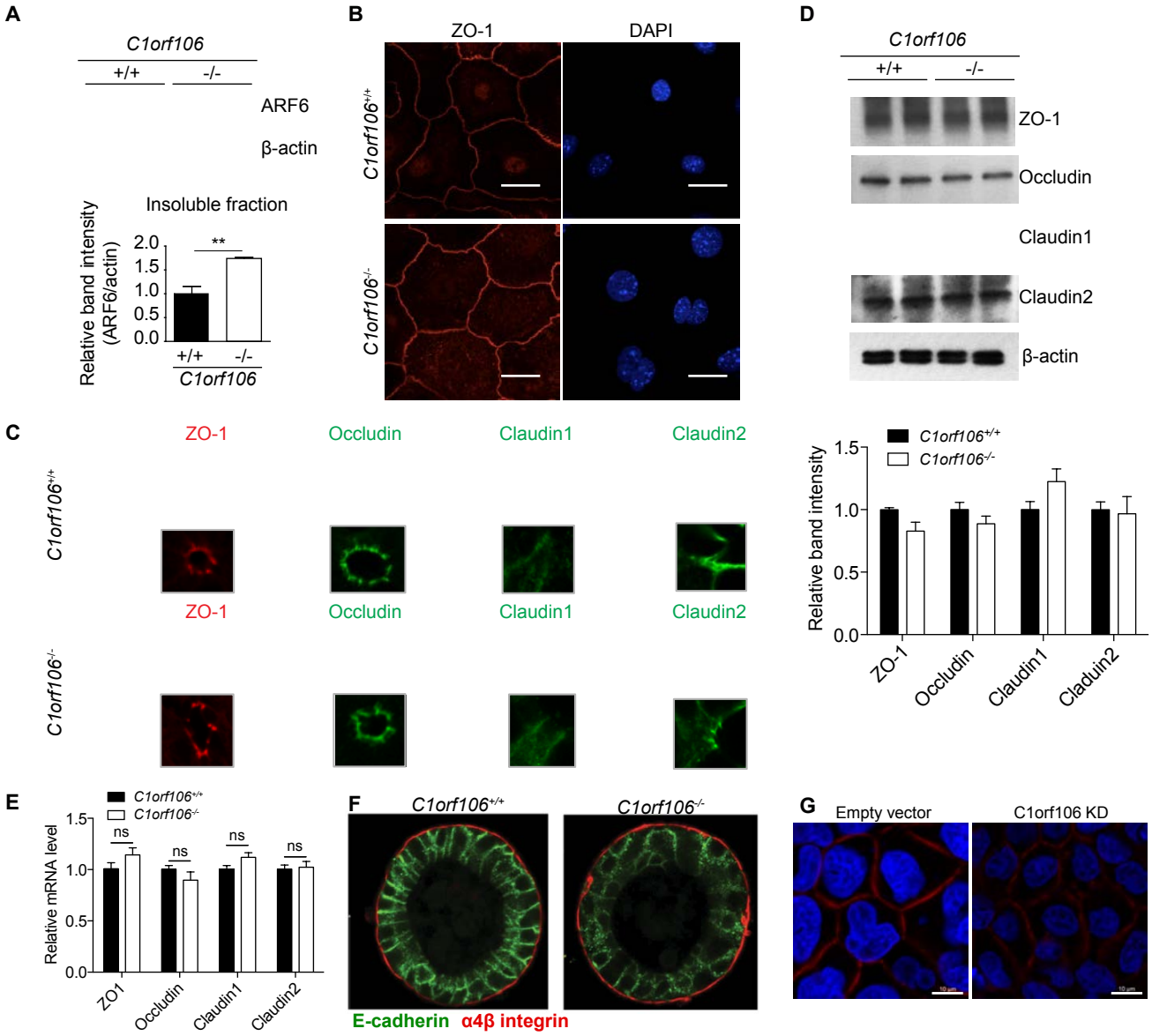

Fig. S6. Increased membrane-associated ARF6 and disorganized E-cadherin in *C1orf106*$^{-/-}$ cells and organoids. (**A**) Immunoblot analysis of intestinal epithelial cells derived from *C1orf106*$^{+/+}$ and *C1orf106*$^{-/-}$ organoids. The insoluble fraction was probed for ARF6. β-actin served as a loading control. ** $P < 0.01$, Student's t test. Error bars indicate SEM. (**B**) Confocal immunofluorescence images of intestinal epithelial monolayers derived from *C1orf106*$^{+/+}$ and *C1orf106*$^{-/-}$ organoids. Cells were stained for ZO-1 and DAPI. Scale bar represents 30μm. (**C**) Confocal immunofluorescence images of sections from *C1orf106*$^{+/+}$ and *C1orf106*$^{-/-}$ mouse colon stained for ZO-1, Occludin, Claudin1, and Claudin2. Scale bar represents 10μm. (**D**) Immunoblot analysis of tight junction proteins in IECs derived from *C1orf106*$^{+/+}$ and *C1orf106*$^{-/-}$ organoids. Quantification of immunoblots is shown below. (**E**) qPCR analysis to estimate the levels of tight junction proteins in IECs derived from *C1orf106*$^{+/+}$ and *C1orf106*$^{-/-}$ organoids. Data are representative of 3 independent experiments. (**F**) Confocal images of colonic organoids from *C1orf106*$^{+/+}$ and *C1orf106*$^{-/-}$ mice stained for E-cadherin (green) and α4β integrin (red). (**G**) Confocal microscopy showing subcellular localization of endogenous E-cadherin in 18-day differentiated Caco-2 cells stably expressing an empty lentiviral vector or shRNA against C1orf106. Scale bars represents 10 μm.

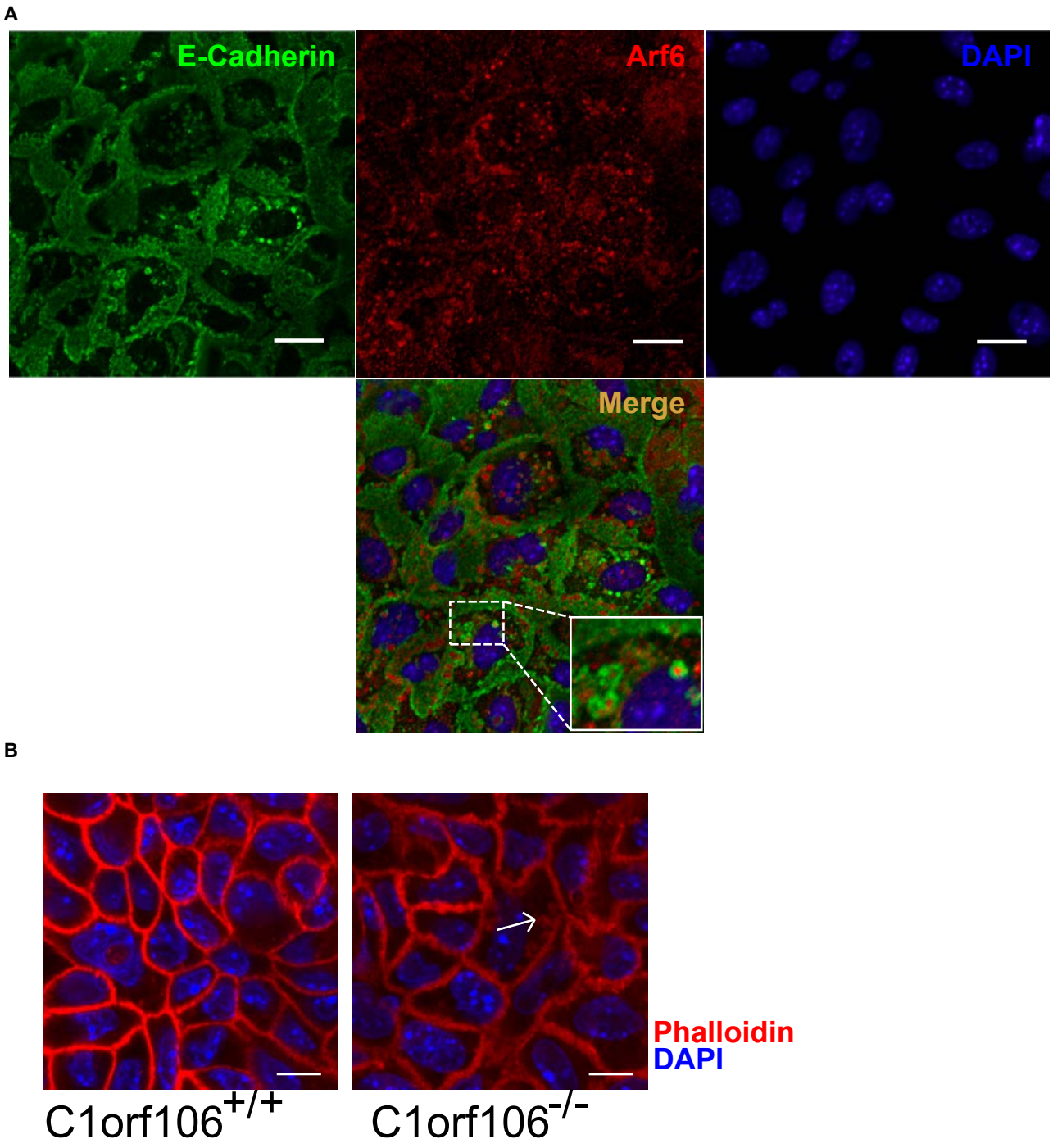

Fig. S7. ARF6 and actin dynamics in *C1orf106*$^{-/-}$ monolayers. (A) Confocal immunofluorescence images of intestinal epithelial cells derived from C1orf106$^{-/-}$ organoids. Cells were stained for ARF6 and E-cadherin. Scale bar represents 10μm. (B) Confocal immunoflourescence images of monolayers derived from colonic C1orf106$^{+/+}$ and C1orf106$^{-/-}$ organiods. Cells were stainined for actin (Phalloidin) and nuclei (DAPI). Scale bar represents 10μm.

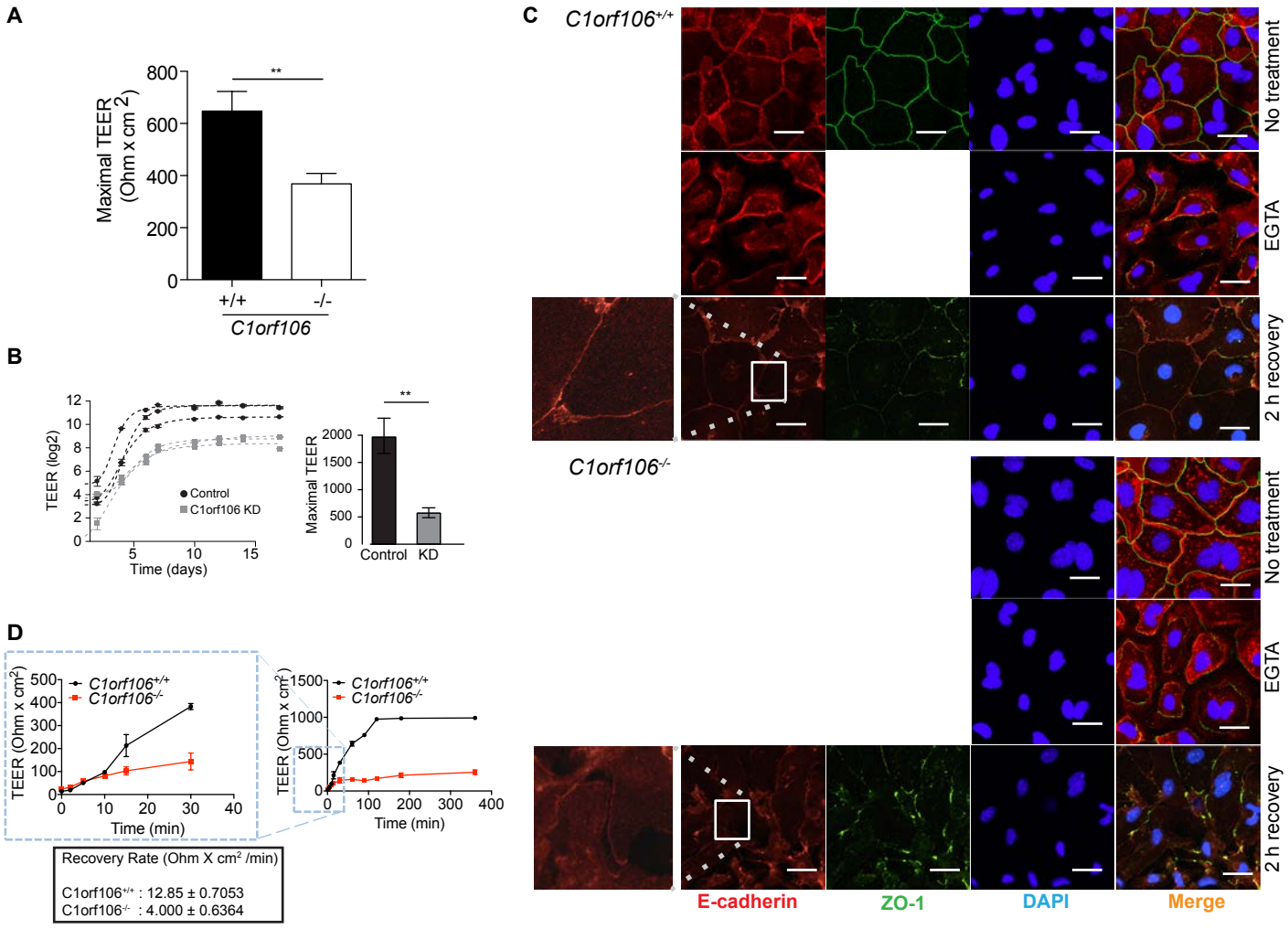

Fig. S8. Recovery of epithelial barrier integrity and E-cadherin after calcium switch is delayed in *C1orf106*$^{-/-}$ monolayers. (**A**) Maximal TEER measurement in IEC monolayers from *C1orf106*$^{+/+}$ and *C1orf106*$^{-/-}$ organoids. Error bar represents mean ± SEM. ** $P < 0.01$, * $P < 0.05$ (Student's t test). (**B**) TEER measurements during epithelial differentiation of Caco-2 cells stably expressing control shRNA or C1orf106 shRNA. A sigmoid (four parameters logistic) curve was fitted to the log(TEER) vs. time for each independent cell line. Data are representative of 3 independent experiments. Error bars indicate SEM. (**C**) Confocal images of organoid-derived monolayers left untreated or treated with 2 mM EGTA for 8 minutes. After EGTA treatment cells were allowed to recover for 2 h. Cells were stained for E-cadherin (red), ZO-1 (green) and nuclei (blue). Scale bar represents 30µm. (**D**) TEER measurement at various time intervals after calcium switch treatment in IEC monolayers from *C1orf106*$^{+/+}$ and *C1orf106*$^{-/-}$ organoids.

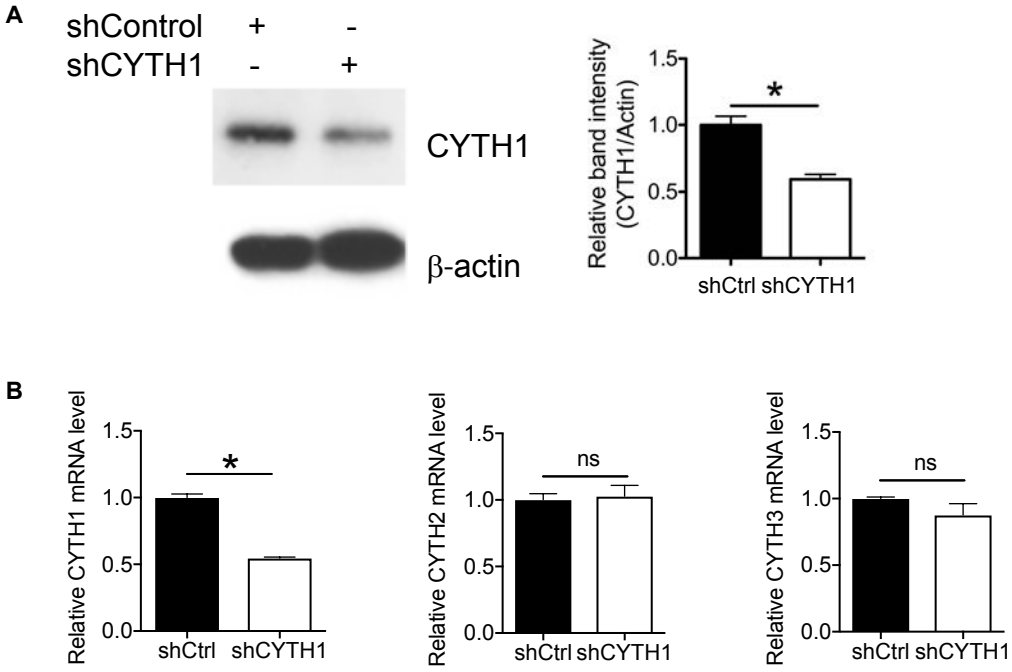

Fig. S9. An shRNA directed against cytohesin-1 gives specific knockdown of cytohesin-1 in *C1orf106*$^{-/-}$ monolayers. (**A**) Immunoblot analysis and quantification of colonic *C1orf106*$^{-/-}$ monolayers transduced with control vector (shControl) or shRNA against cytohesin-1 and probed for cytohesin-1. β-actin served as loading control. *$P < 0.05$, Student's t test. Data is representative of 3 independent experiments. (**B**) qRT-PCR analysis of CYTH1, CYTH2, and CYTH3 in *C1orf106*$^{-/-}$ monolayers transduced with control vector (shControl) or shRNA against cytohesin-1.

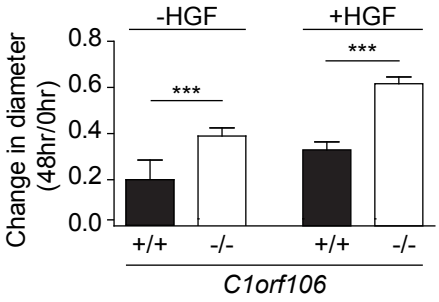

Fig. S10. Loss of *C1orf106* increases cell motility. Quantification of cell migration in organoid-derived colonic monolayers after 48 h with or without HGF treatment. Error bar represents mean ± SEM. *** $P < 0.001$, ** $P < 0.01$, * $P < 0.05$ (Student's t test).

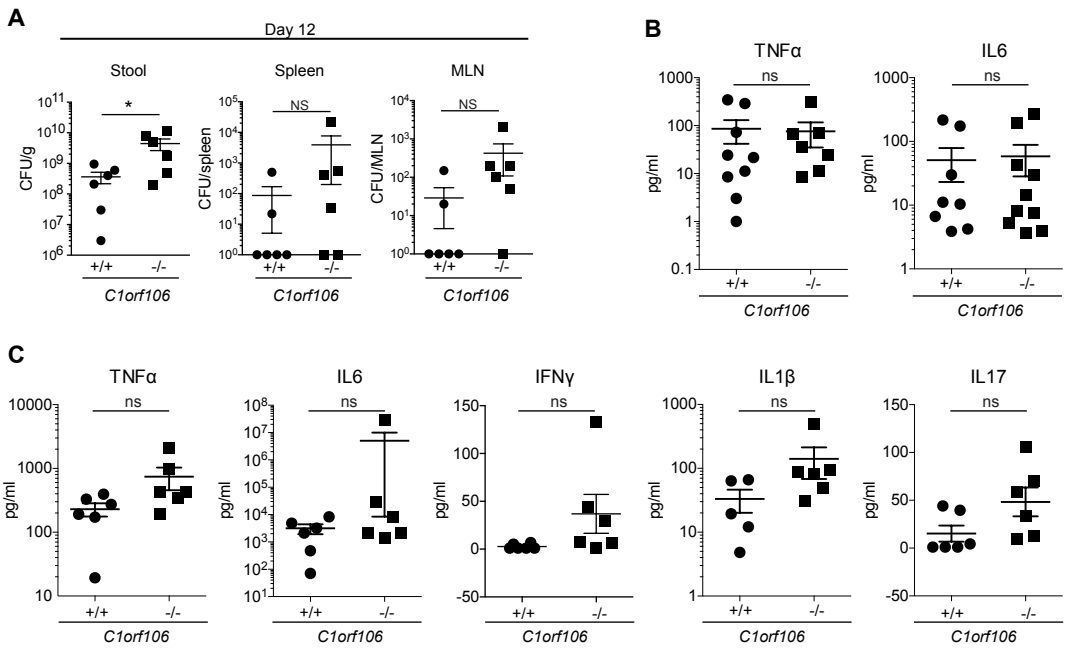

Fig. S11. Loss of *C1orf106* does not increase cytokine production following *Citrobacter rodentium* infection *in vivo*. (**A**) Stool, spleen, and MLN CFU measured at 12 days post-infection with *C. rodentium*. (**B**) Cytometric bead array was performed on media collected from colon sections from *Citrobacter rodentium*-infected *C1orf106*$^{+/+}$ and *C1orf106*$^{-/-}$ mice at 5 days post-infection to quantitate levels of TNFα and IL-6. Error bars represent SEM. (**C**) Cytometric bead array was performed on media collected from colon sections from *Citrobacter rodentium*-infected *C1orf106*$^{+/+}$ and *C1orf106*$^{-/-}$ mice at 12 days post-infection to quantitate levels of TNFα, IL-6, IFNγ, IL1β, and IL17. *$P < 0.05$ (Student's t test). Error bars ± SEM. N = 6 mice per genotype in at least 2 independent experiments.

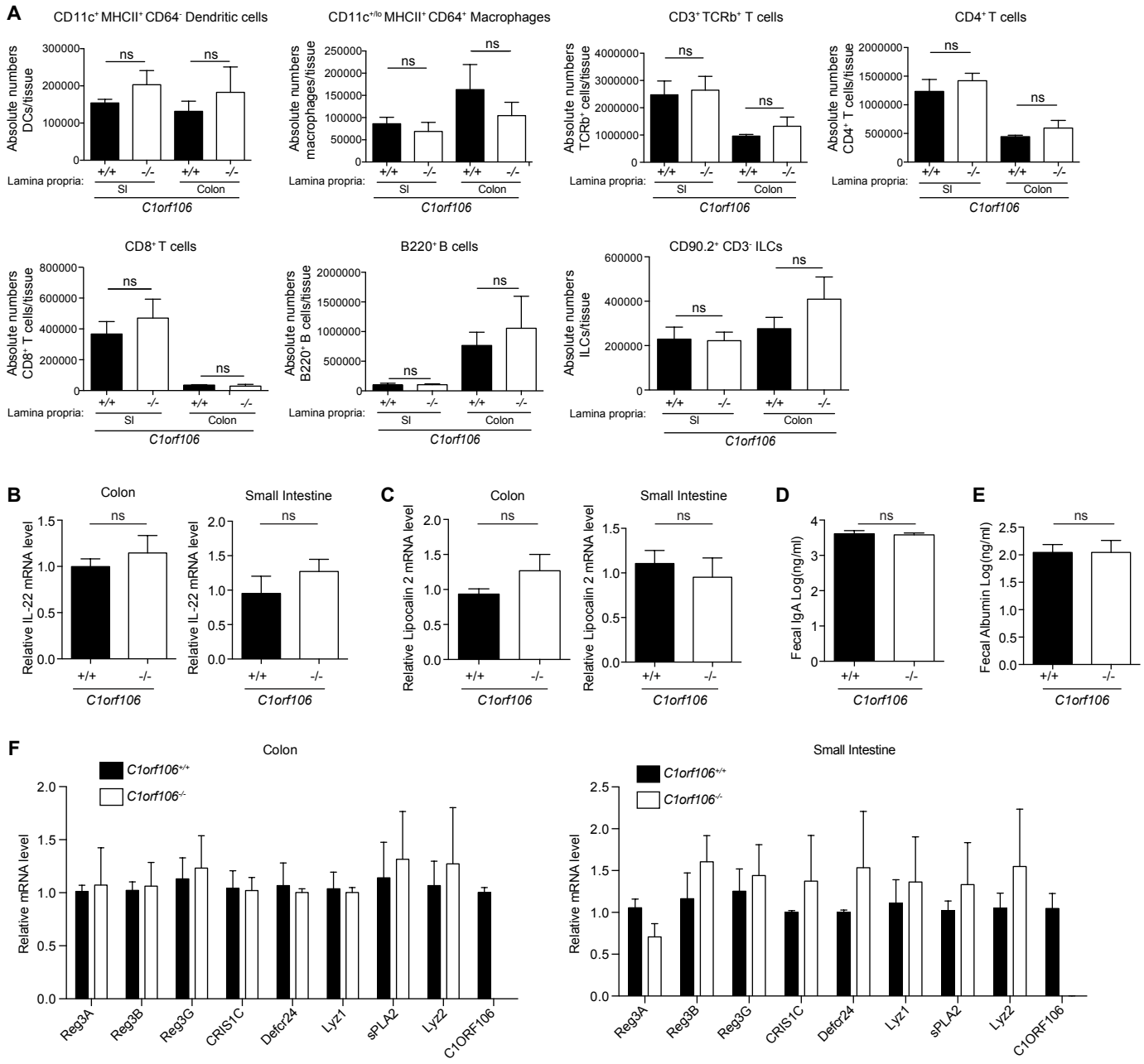

Fig. S12. Baseline quantification of immune cell types, inflammation and antimicrobial peptide levels in C1orf106$^{+/+}$ and C1orf106$^{-/-}$ mice.(A) Immunophenotyping in lamina propria cells isolated from C1orf106$^{+/+}$ and C1orf106$^{-/-}$ mice. Error bars ± SEM. Student's t test. N = 3 mice per genotype. (**B**) qRT-PCR analysis of IL-22 in the distal colon and small intestine sections of C1orf106$^{+/+}$ and C1orf106$^{-/-}$ mice. Data are representative of 3 independent experiments. (**C**) qRT-PCR analysis of Lipocalin 2 in the distal colon and small intestine sections of C1orf106$^{+/+}$ and C1orf106$^{-/-}$ mice. Data are representative of 3 independent experiments. (**D**) ELISA quantification of fecal IgA level. Data are representative of 3 independent experiments. (**E**) ELISA quantification of fecal albumin levels. Data are representative of 3 independent experiments. (**F**) qRT-PCR analysis of mouse antimicrobial peptides in distal colon and small intestine sections of C1orf106$^{+/+}$ and C1orf106$^{-/-}$ mice. Error bars ± SEM. Data are representative of 3 independent experiments.

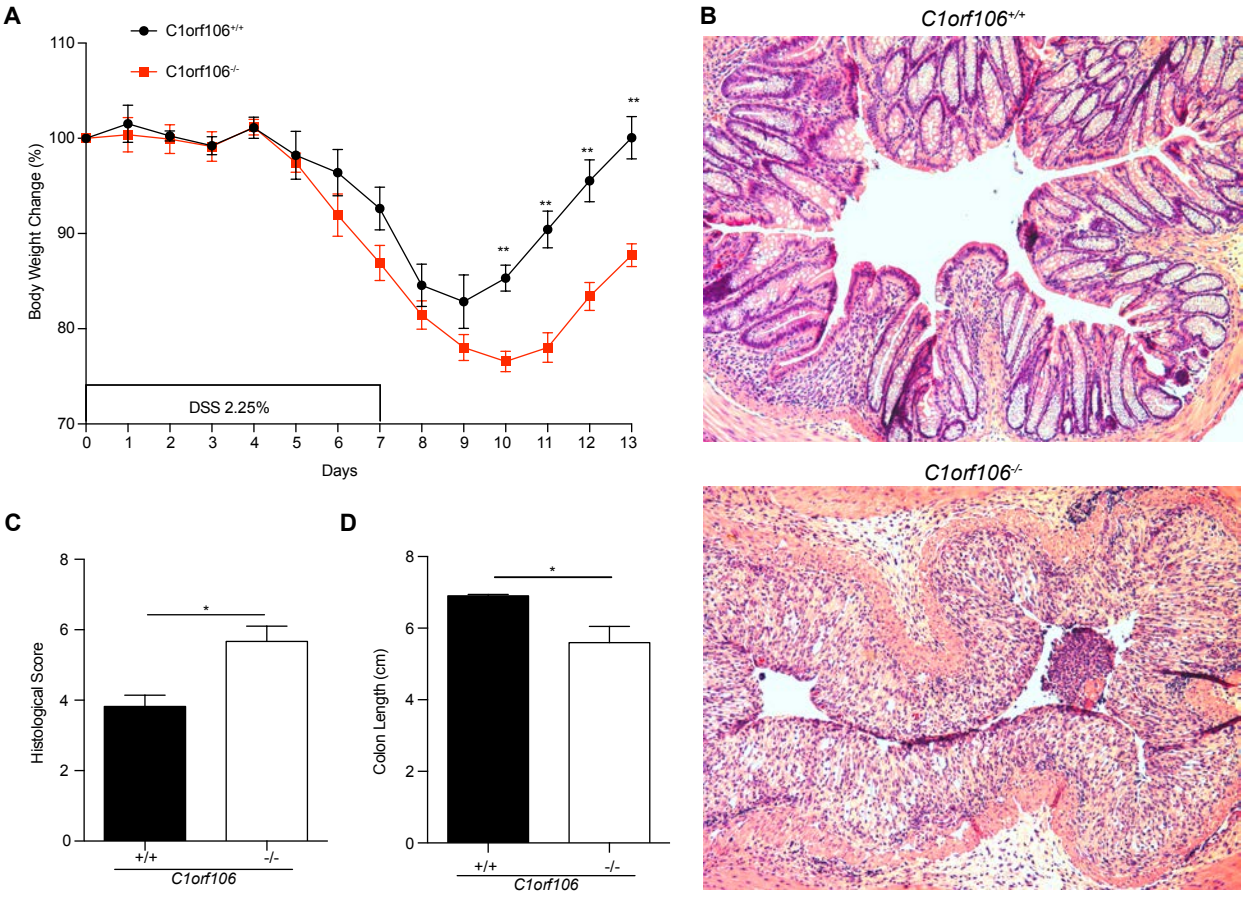

Fig. S13. Loss of *C1orf106* leads to increased susceptibility to DSS treatment. (A) Percentage body weight change measured during DSS treatment and the recovery phase. *P < 0.05, **P < 0.01 (Student's t test). Error bars ± SEM. Data are representative of at least two experiments. (B) H & E-stained sections of colon from C1orf106$^{+/+}$ and C1orf106$^{-/-}$ mice treated with 2.25% DSS at day 13. (C) Colonic histopathology score measured on day 13 after DSS treatment. *P < 0.05 (Student's t test). Error bars ± SEM. Data are representative of at least two experiments. (D) Colon length of C1orf106$^{+/+}$ and C1orf106$^{-/-}$ mice treated with 2.25% DSS at day 13. *P < 0.05 (Student's t test). Error bars ± SEM. Data are representative of at least two experiments.

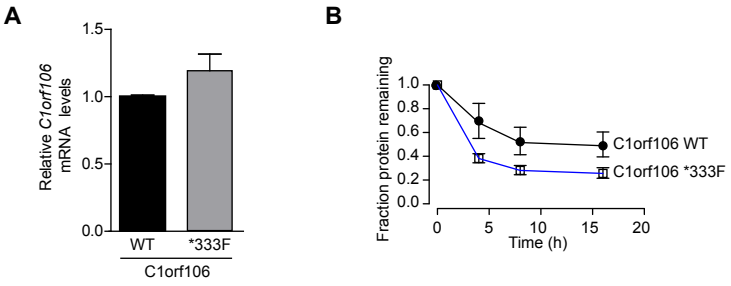

Fig. S14. No difference in mRNA expression of C1orf106 variants despite decrease in protein levels over time. (**A**) Relative mRNA levels of C1orf106 WT and C1orf106 *333F in HEK293T cells transfected with WT-C1orf106-V5 and *333F-C1orf106-V5 plasmids respectively. Error bars represent SD. (**B**) LS174T cells stably overexpressing C1orf106 WT and C1orf106 *333F were treated with 50 μg/ml cycloheximide for the indicated times. After immunoblot analysis, densitometry was performed and results were graphed as relative C1orf106 levels normalized to β-actin. The fraction of protein remaining represents the geometric mean +/- SEM of seven measurements in 4 independent experiments.

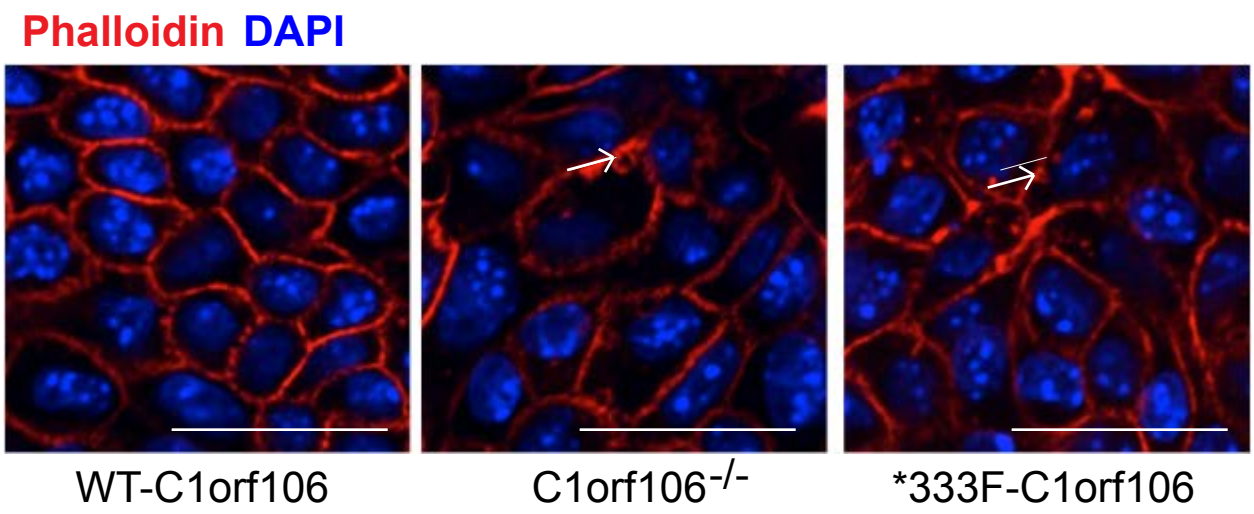

Fig. S15. Confocal immunofluorescence images of monolayers derived from C1orf106$^{-/-}$, C1orf106 WT, and C1orf106*333F organoids. Cells were stained for actin (Phalloidin) and nuclei (DAPI). Scale bar represents 50μm.

References and Notes

1. B. Khor, A. Gardet, R. J. Xavier, Genetics and pathogenesis of inflammatory bowel disease. *Nature* **474**, 307–317 (2011). doi:10.1038/nature10209 Medline

2. J. Mankertz, J. D. Schulzke, Altered permeability in inflammatory bowel disease: Pathophysiology and clinical implications. *Curr. Opin. Gastroenterol.* **23**, 379–383 (2007). doi:10.1097/MOG.0b013e32816aa392 Medline

3. D. Hollander, C. M. Vadheim, E. Brettholz, G. M. Petersen, T. Delahunty, J. I. Rotter, Increased intestinal permeability in patients with Crohn's disease and their relatives. A possible etiologic factor. *Ann. Intern. Med.* **105**, 883–885 (1986). doi:10.7326/0003-4819-105-6-883 Medline

4. C. A. Anderson, G. Boucher, C. W. Lees, A. Franke, M. D'Amato, K. D. Taylor, J. C. Lee, P. Goyette, M. Imielinski, A. Latiano, C. Lagacé, R. Scott, L. Amininejad, S. Bumpstead, L. Baidoo, R. N. Baldassano, M. Barclay, T. M. Bayless, S. Brand, C. Büning, J.-F. Colombel, L. A. Denson, M. De Vos, M. Dubinsky, C. Edwards, D. Ellinghaus, R. S. N. Fehrmann, J. A. B. Floyd, T. Florin, D. Franchimont, L. Franke, M. Georges, J. Glas, N. L. Glazer, S. L. Guthery, T. Haritunians, N. K. Hayward, J.-P. Hugot, G. Jobin, D. Laukens, I. Lawrance, M. Lémann, A. Levine, C. Libioulle, E. Louis, D. P. McGovern, M. Milla, G. W. Montgomery, K. I. Morley, C. Mowat, A. Ng, W. Newman, R. A. Ophoff, L. Papi, O. Palmieri, L. Peyrin-Biroulet, J. Panés, A. Phillips, N. J. Prescott, D. D. Proctor, R. Roberts, R. Russell, P. Rutgeerts, J. Sanderson, M. Sans, P. Schumm, F. Seibold, Y. Sharma, L. A. Simms, M. Seielstad, A. H. Steinhart, S. R. Targan, L. H. van den Berg, M. Vatn, H. Verspaget, T. Walters, C. Wijmenga, D. C. Wilson, H.-J. Westra, R. J. Xavier, Z. Z. Zhao, C. Y. Ponsioen, V. Andersen, L. Torkvist, M. Gazouli, N. P. Anagnou, T. H. Karlsen, L. Kupcinskas, J. Sventoraityte, J. C. Mansfield, S. Kugathasan, M. S. Silverberg, J. Halfvarson, J. I. Rotter, C. G. Mathew, A. M. Griffiths, R. Gearry, T. Ahmad, S. R. Brant, M. Chamaillard, J. Satsangi, J. H. Cho, S. Schreiber, M. J. Daly, J. C. Barrett, M. Parkes, V. Annese, H. Hakonarson, G. Radford-Smith, R. H. Duerr, S. Vermeire, R. K. Weersma, J. D. Rioux, Meta-analysis identifies 29 additional ulcerative colitis risk loci, increasing the number of confirmed associations to 47. *Nat. Genet.* **43**, 246–252 (2011). doi:10.1038/ng.764 Medline

5. M. A. Rivas, M. Beaudoin, A. Gardet, C. Stevens, Y. Sharma, C. K. Zhang, G. Boucher, S. Ripke, D. Ellinghaus, N. Burtt, T. Fennell, A. Kirby, A. Latiano, P. Goyette, T. Green, J. Halfvarson, T. Haritunians, J. M. Korn, F. Kuruvilla, C. Lagacé, B. Neale, K. S. Lo, P. Schumm, L. Törkvist, National Institute of Diabetes and Digestive Kidney Diseases Inflammatory Bowel Disease Genetics Consortium (NIDDK IBDGC), United Kingdom Inflammatory Bowel Disease Genetics Consortium, International Inflammatory Bowel Disease Genetics Consortium, M. C. Dubinsky, S. R. Brant, M. S. Silverberg, R. H. Duerr, D. Altshuler, S. Gabriel, G. Lettre, A. Franke, M. D'Amato, D. P. B. McGovern, J. H. Cho, J. D. Rioux, R. J. Xavier, M. J. Daly, Deep resequencing of GWAS loci identifies independent rare variants associated with inflammatory bowel disease. *Nat. Genet.* **43**, 1066–1073 (2011). doi:10.1038/ng.952 Medline

6. Y. Liu, H. Xu, S. Chen, X. Chen, Z. Zhang, Z. Zhu, X. Qin, L. Hu, J. Zhu, G.-P. Zhao, X. Kong, Genome-wide interaction-based association analysis identified multiple new

susceptibility loci for common diseases. *PLOS Genet.* **7**, e1001338 (2011). doi:10.1371/journal.pgen.1001338 Medline

7. J. E. Casanova, Regulation of Arf activation: The Sec7 family of guanine nucleotide exchange factors. *Traffic* **8**, 1476–1485 (2007). doi:10.1111/j.1600-0854.2007.00634.x Medline

8. J. G. Donaldson, C. L. Jackson, ARF family G proteins and their regulators: Roles in membrane transport, development and disease. *Nat. Rev. Mol. Cell Biol.* **12**, 362–375 (2011). doi:10.1038/nrm3117 Medline

9. D. Frescas, M. Pagano, Deregulated proteolysis by the F-box proteins SKP2 and β-TrCP: Tipping the scales of cancer. *Nat. Rev. Cancer* **8**, 438–449 (2008). doi:10.1038/nrc2396 Medline

10. J. R. Skaar, J. K. Pagan, M. Pagano, Mechanisms and function of substrate recruitment by F-box proteins. *Nat. Rev. Mol. Cell Biol.* **14**, 369–381 (2013). doi:10.1038/nrm3582 Medline

11. T. A. Soucy, P. G. Smith, M. A. Milhollen, A. J. Berger, J. M. Gavin, S. Adhikari, J. E. Brownell, K. E. Burke, D. P. Cardin, S. Critchley, C. A. Cullis, A. Doucette, J. J. Garnsey, J. L. Gaulin, R. E. Gershman, A. R. Lublinsky, A. McDonald, H. Mizutani, U. Narayanan, E. J. Olhava, S. Peluso, M. Rezaei, M. D. Sintchak, T. Talreja, M. P. Thomas, T. Traore, S. Vyskocil, G. S. Weatherhead, J. Yu, J. Zhang, L. R. Dick, C. F. Claiborne, M. Rolfe, J. B. Bolen, S. P. Langston, An inhibitor of NEDD8-activating enzyme as a new approach to treat cancer. *Nature* **458**, 732–736 (2009). doi:10.1038/nature07884 Medline

12. W. Kolanus, Guanine nucleotide exchange factors of the cytohesin family and their roles in signal transduction. *Immunol. Rev.* **218**, 102–113 (2007). doi:10.1111/j.1600-065X.2007.00542.x Medline

13. F. Palacios, L. Price, J. Schweitzer, J. G. Collard, C. D'Souza-Schorey, An essential role for ARF6-regulated membrane traffic in adherens junction turnover and epithelial cell migration. *EMBO J.* **20**, 4973–4986 (2001). doi:10.1093/emboj/20.17.4973 Medline

14. T. J. Harris, U. Tepass, Adherens junctions: From molecules to morphogenesis. *Nat. Rev. Mol. Cell Biol.* **11**, 502–514 (2010). doi:10.1038/nrm2927 Medline

15. L. Shen, C. R. Weber, D. R. Raleigh, D. Yu, J. R. Turner, Tight junction pore and leak pathways: A dynamic duo. *Annu. Rev. Physiol.* **73**, 283–309 (2011). doi:10.1146/annurev-physiol-012110-142150 Medline

16. G. Swaminathan, C. A. Cartwright, Rack1 promotes epithelial cell-cell adhesion by regulating E-cadherin endocytosis. *Oncogene* **31**, 376–389 (2012). doi:10.1038/onc.2011.242 Medline

17. D. Knights, K. G. Lassen, R. J. Xavier, Advances in inflammatory bowel disease pathogenesis: Linking host genetics and the microbiome. *Gut* **62**, 1505–1510 (2013). doi:10.1136/gutjnl-2012-303954 Medline

18. S. Nell, S. Suerbaum, C. Josenhans, The impact of the microbiota on the pathogenesis of IBD: Lessons from mouse infection models. *Nat. Rev. Microbiol.* **8**, 564–577 (2010). doi:10.1038/nrmicro2403 Medline

19. UK IBD Genetics Consortium, Wellcome Trust Case Control Consortium 2, Genome-wide association study of ulcerative colitis identifies three new susceptibility loci, including the HNF4A region. *Nat. Genet.* **41**, 1330–1334 (2009). doi:10.1038/ng.483 Medline

20. J. Rappsilber, M. Mann, Y. Ishihama, Protocol for micro-purification, enrichment, pre-fractionation and storage of peptides for proteomics using StageTips. *Nat. Protoc.* **2**, 1896–1906 (2007). doi:10.1038/nprot.2007.261 Medline

21. N. D. Udeshi, T. Svinkina, P. Mertins, E. Kuhn, D. R. Mani, J. W. Qiao, S. A. Carr, Refined preparation and use of anti-diglycine remnant (K-ε-GG) antibody enables routine quantification of 10,000s of ubiquitination sites in single proteomics experiments. *Mol. Cell. Proteomics* **12**, 825–831 (2013). doi:10.1074/mcp.O112.027094 Medline

22. J. Gupta, I. del Barco Barrantes, A. Igea, S. Sakellariou, I. S. Pateras, V. G. Gorgoulis, A. R. Nebreda, Dual function of p38α MAPK in colon cancer: Suppression of colitis-associated tumor initiation but requirement for cancer cell survival. *Cancer Cell* **25**, 484–500 (2014). doi:10.1016/j.ccr.2014.02.019 Medline

23. P. Artursson, Epithelial transport of drugs in cell culture. I: A model for studying the passive diffusion of drugs over intestinal absorptive (Caco-2) cells. *J. Pharm. Sci.* **79**, 476–482 (1990). doi:10.1002/jps.2600790604 Medline

24. C. F. Krieglstein, C. Anthoni, W. H. Cerwinka, K. Y. Stokes, J. Russell, M. B. Grisham, D. N. Granger, Role of blood- and tissue-associated inducible nitric-oxide synthase in colonic inflammation. *Am. J. Pathol.* **170**, 490–496 (2007). doi:10.2353/ajpath.2007.060594 Medline

25. K. Kabashima, T. Saji, T. Murata, M. Nagamachi, T. Matsuoka, E. Segi, K. Tsuboi, Y. Sugimoto, T. Kobayashi, Y. Miyachi, A. Ichikawa, S. Narumiya, The prostaglandin receptor EP4 suppresses colitis, mucosal damage and CD4 cell activation in the gut. *J. Clin. Invest.* **109**, 883–893 (2002). doi:10.1172/JCI0214459 Medline

26. H. Miyoshi, T. S. Stappenbeck, In vitro expansion and genetic modification of gastrointestinal stem cells in spheroid culture. *Nat. Protoc.* **8**, 2471–2482 (2013). doi:10.1038/nprot.2013.153 Medline

27. C. Moon, K. L. VanDussen, H. Miyoshi, T. S. Stappenbeck, Development of a primary mouse intestinal epithelial cell monolayer culture system to evaluate factors that modulate IgA transcytosis. *Mucosal Immunol.* **7**, 818–828 (2014). doi:10.1038/mi.2013.98 Medline

28. B. K. Koo, D. E. Stange, T. Sato, W. Karthaus, H. F. Farin, M. Huch, J. H. van Es, H. Clevers, Controlled gene expression in primary Lgr5 organoid cultures. *Nat. Methods* **9**, 81–83 (2011). doi:10.1038/nmeth.1802 Medline